

Figure 5: Phenomenological parametrisation of the rapidity distributions at (left) $\sqrt{s_{\text{NN}}} = 110.4 \text{ GeV}$ ($p\text{Ar}$) and (right) $\sqrt{s_{\text{NN}}} = 86.6 \text{ GeV}$ ($p\text{He}$). The binning schemes corresponds to those used in the analysis. The curves are normalised to unity for y^* within $[-3.5, 3.5]$.

Supplementary material for LHCb-PAPER-2018-023

Smooth distributions of phenomenological predictions

The phenomenological distributions used in the article are based on the parametrisations given in Ref. [49] for the rapidity distributions and Ref. [11] for the transverse momentum distributions. For rapidity and transverse momentum, the solid and dashed red lines of Fig. 3 and Fig. 4 of the paper are obtained with linear and logarithmic interpolations, respectively, between the results from the E789 ($p\text{Au}$, $\sqrt{s_{\text{NN}}} = 38.7 \text{ GeV}$) [50], the HERA-B ($p\text{C}$, $\sqrt{s_{\text{NN}}} = 41.5 \text{ GeV}$) [51] and the PHENIX (pp , $\sqrt{s} = 200 \text{ GeV}$) [52] experiments.

The rapidity distribution is given by

$$\frac{dN_{J/\psi}}{dy^*} = \frac{1}{I_{y^*}} \left(1 - \frac{2M_{\text{T}}}{\sqrt{s}} \cosh(y^*) \right)^n$$

where the parameters have been provided by the authors of [11, 49]. $M_{\text{T}} = \sqrt{M^2 + p_{\text{T}}^2}$ (where M_{T} is the transverse mass) with $M = 3.1 \text{ GeV}/c^2$ and $p_{\text{T}} = 1 \text{ GeV}/c$, and

- at 86.6 GeV, linear (logarithmic) interpolation: $n = 6.4$ (6.9)
- at 110.4 GeV, linear (logarithmic) interpolation: $n = 6.8$ (7.3)

and I_{y^*} is the normalisation factor of the function integrated over $-3.5 < y^* < 3.5$. Figure 5 shows the phenomenological curves at both $p\text{Ar}$ and $p\text{He}$ centre-of-mass energies. The same binning scheme as in the letter is used.

The transverse momentum distribution is given by

$$\frac{dN_{J/\psi}}{dp_{\text{T}}} = \frac{1}{I_{p_{\text{T}}}} \left(\frac{p_0^2 + p_{\text{T}}^2}{p_0^2} \right)^{-m} = \frac{1}{I_{p_{\text{T}}}} \left(1 + \frac{p_{\text{T}}^2}{p_0^2} \right)^{-m}$$

where the parameters have been provided by the authors of Refs. [11, 49]: $p_0 = 3.2 \text{ GeV}/c$ and

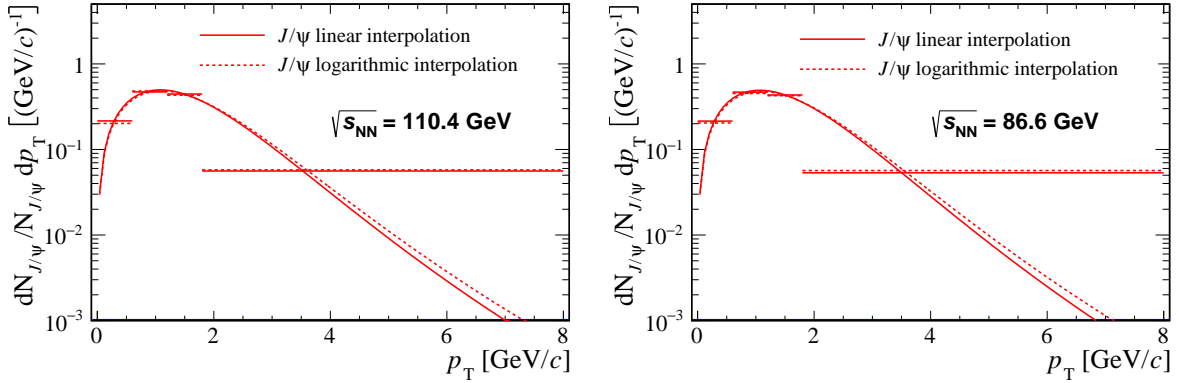


Figure 6: Phenomenological parametrisation of the transverse momentum distributions at (left) $\sqrt{s_{\text{NN}}} = 110.4 \text{ GeV}$ ($p\text{Ar}$) and (right) $\sqrt{s_{\text{NN}}} = 86.6 \text{ GeV}$ ($p\text{He}$). The binning schemes corresponds to those in the analysis. The curves are normalised to unity for p_{T} within $[0, 8] \text{ GeV}/c$.

354 • at 86.6 GeV, linear (logarithmic) interpolation: $m = 5.0$ (4.8)

355 • at 110.4 GeV, linear (logarithmic) interpolation: $m = 4.9$ (4.7)

356 and $I_{p_{\text{T}}}$ is the normalisation factor of the function integrated over $0 < p_{\text{T}} < 8 \text{ GeV}/c$.

357 Figure 6 shows the phenomenological curves at both $p\text{Ar}$ and $p\text{He}$ centre-of-mass energies.

358 The same binning scheme as in the letter is used.

359 Potential effects related to polarisation

360 The detection efficiency is affected by the J/ψ polarisation, especially by the longitudinal
361 polarisation parameter λ_{θ} which is defined as follows,

$$\frac{d^2 N}{d \cos \theta d \Phi} \propto 1 + \lambda_{\theta} \cos^2 \theta + \lambda_{\theta \Phi} \sin 2\theta \cos \Phi + \lambda_{\Phi} \sin^2 \theta \cos 2\Phi, \quad (2)$$

362 where, in the helicity frame, $d^2 N/d \cos \theta d \Phi$ is the angular distribution of muons in the
363 $J/\psi \rightarrow \mu^+ \mu^-$ decays, θ is the polar angle between the direction of the positive lepton and
364 the flight direction of the J/ψ in the centre-of-mass frame of the colliding hadrons, and Φ is
365 the azimuthal angle, measured with respect to the production plane. Since the production
366 plane is uniformly distributed in azimuthal angle, only the θ dependence described by
367 the parameter λ_{θ} has an effect on the efficiency. A value of $\lambda_{\theta} = 0$ refers to unpolarised
368 J/ψ mesons, while $\lambda_{\theta} > 0$ describes transverse polarisation ($J_z = \pm 1$ enhanced) and
369 $\lambda_{\theta} < 0$ longitudinal polarisation ($J_z = 0$ enhanced). Zero polarisation is assumed in this
370 letter. In order to facilitate the extrapolation of the cross-sections measured assuming
371 zero polarisation to other polarisation values, the increase of the total efficiency of the
372 J/ψ meson for a longitudinal polarisation corresponding to $\lambda_{\theta} = -0.2$ [31], compared to
373 zero polarisation, is given in Ref. [35]. These numbers have been computed based on the
374 analysis performed in Ref. [34]. The relative change in efficiency is linear, to 5% accuracy,
375 between $\lambda_{\theta} = 0$ and $\lambda_{\theta} = -0.2$.